In vivo reconstitution of autophagy in *Saccharomyces cerevisiae*

Yang Cao, Heesun Cheong, Hui Song, and Daniel J. Klionsky

Life Sciences Institute, Department of Biological Chemistry, and Department of Molecular, Cellular and Developmental Biology, University of Michigan, Ann Arbor, MI 48109

Autophagy is a major intracellular degradative pathway that is involved in various human diseases. The role of autophagy, however, is complex; although the process is generally considered to be cytoprotective, it can also contribute to cellular dysfunction and disease progression. Much progress has been made in our understanding of autophagy, aided in large part by the identification of the *autophagy*-related (*ATG*) genes. Nonetheless, our understanding of the molecular mechanism remains limited. In this study, we generated a *Saccharomyces cerevisiae* multiple-knockout strain with 24 *ATG* genes deleted, and we used it to carry out an in vivo reconstitution of the autophagy pathway. We determined minimum requirements for different aspects of autophagy and studied the initial protein assembly steps at the phagophore assembly site. In vivo reconstitution enables the study of autophagy within the context of the complex regulatory networks that control this process, an analysis that is not possible with an in vitro system.

Introduction

Macroautophagy (hereafter autophagy) is a conserved degradative pathway in eukaryotic cells that also plays an essential role in development and differentiation and has been implicated in many human diseases (Levine and Klionsky, 2004; Mizushima, 2007). Autophagy involves de novo formation of a double-membrane vesicle (the autophagosome) in the cytosol, fusion of this vesicle with the lysosome/vacuole, and the subsequent breakdown and recycling of the cargo. With the identification of *autophagy*-related (*ATG*) genes in yeast, autophagy research has shifted from morphological analyses to the understanding of molecular mechanisms (Klionsky, 2007). 31 *ATG* genes have been identified in baker's and methylotrophic yeasts, and many of them have homologues in higher eukaryotes (Rubinsztein et al., 2007).

Autophagy is generally considered to be nonselective, but there are also selective types of autophagy. The cytoplasm-to-vacuole targeting (Cvt) pathway is an example of selective autophagy wherein the precursor form of the resident vacuolar hydrolase aminopeptidase I (prApe1) is selectively transported from the cytoplasm into the vacuole under vegetative conditions (Klionsky, 2005). The Cvt pathway shares most of the components needed for autophagy but utilizes additional proteins in cargo recognition and packaging. After synthesis in the cytosol, prApe1 forms an oligomer, which is targeted through a receptor, Atg19, and an adaptor, Atg11 (Kim et al., 1997; Scott et al., 2001; Shintani et al., 2002; Shintani and Klionsky, 2004; Yorimitsu and Klionsky, 2005). There is no evidence that the Cvt pathway exists outside of fungi. However, a similar recognition mechanism might be used in mammalian examples of selective autophagy (Iwata et al., 2006).

Most of the Atg proteins at least transiently colocalize at the phagophore assembly site (PAS; the presumed nucleating site of the autophagosome) in both the Cvt pathway and nonselective autophagy; however, this site is poorly defined and characterized. Knowing how Atg proteins are targeted to the PAS will help us dissect the vesicle formation process and understand how these proteins interact and function. The cargo complex including Atg11 is the initial component for PAS assembly in vegetative conditions (Shintani et al., 2002), whereas Atg17 has been shown to be an initial factor for PAS assembly in starvation (Suzuki et al., 2007). Components in the Atg17 complex, such as Atg1 and Atg13, are also involved in organizing the PAS during starvation (Cheong et al., 2008; Kawamata et al., 2008). However, many questions regarding the temporal order of protein assembly at the PAS still remain.

Correspondence to Daniel J. Klionsky: klionsky@umich.edu

Abbreviations used in this paper: Ape1, aminopeptidase I; ATG, *autophagy* related; Cps1, carboxypeptidase S; Cvt, cytoplasm-to-vacuole targeting; MKO, multiple knockout; MVB, multivesicular body; PAS, phagophore assembly site; PE, phosphatidylethanolamine; Pgk1, phosphoglycerate kinase.

The Rockefeller University Press $30.00
J. Cell Biol. 182 No. 4 703–713
www.jcb.org/cgi/doi/10.1083/jcb.200801035

Among the conserved genes, eight participate in two separate but related conjugation systems involving two ubiquitin-like proteins, Atg8 and Atg12. Atg8 is conjugated to phosphatidylethanolamine (PE) through the serial action of Atg4, Atg7, and Atg3 (Ichimura et al., 2000). The C-terminal arginine residue of Atg8 is first removed by the cysteine protease Atg4, exposing a glycine residue that is now accessible to the E1-like activating enzyme Atg7. The activated Atg8 is then transferred to the E2-like conjugating enzyme Atg3 and finally conjugated to PE. Atg8 can be deconjugated from Atg8–PE through a second cleavage by Atg4, although the mechanism that regulates the timing of Atg4 cleavage is not known. The second ubiquitin-like protein, Atg12, is covalently linked to Atg5 through the action of the E1-like Atg7 and an E2-like enzyme, Atg10 (Mizushima et al., 1998). The Atg12–Atg5 conjugate also binds another protein, Atg16, whose oligomerization leads to a tetrameric complex of Atg12–Atg5-Atg16 (Mizushima et al., 1999; Kuma et al., 2002). The Atg8–PE level is reduced in the absence of Atg12, Atg5, or Atg16, and the Atg12–Atg5 conjugate may act as an E3-like enzyme in the Atg8–PE conjugation system (Suzuki et al., 2001; Hanada et al., 2007). However, the efficiency of Atg12–Atg5 conjugation is apparently not affected by the Atg8–PE system (Kuma et al., 2002). Although in vitro reconstitution of both Atg8–PE and Atg12–Atg5 conjugation has been described previously (Ichimura et al., 2004; Hanada et al., 2007; Shao et al., 2007; Fujioka et al., 2008), in vivo reconstitution of the two reactions in eukaryotic cells is not available. Thus, the physiological significance of some of the in vitro observations has not been verified.

Many steps of autophagy have been analyzed in vivo using standard molecular genetics in single- and double-deletion mutant strains, and a smaller subset of the reactions have been reconstituted in vitro. It is unlikely that the entire process will be reconstituted in vitro in the near term because of the complexity of the system and the lack of knowledge regarding basic issues, such as the origin of the sequestering membrane. In addition, in vitro studies inherently lack many critical elements such as the cytoskeleton and the regulatory controls that play important roles in vivo. To provide a physiological reconstitution system, we deleted 24 *ATG* genes directly required for autophagy and/or the Cvt pathway using a multiple knockout (MKO) strategy. We used this MKO strain to determine the minimum requirements for cargo packaging, initial assembly of the starvation-specific PAS, and conjugation of the ubiquitin-like Atg proteins. Our results with the MKO strain verify the role of particular Atg proteins in cargo packaging, and extend previous studies on PAS assembly and protein conjugation that were based on work with individual or double-deletion strains and/or in vitro studies. With this work, we present a new method to tackle complex cellular pathways, particularly those with extensive regulatory networks such as autophagy that cannot be easily replicated in vitro.

Results

Construction of a MKO strain to study autophagy

We were able to construct the MKO strain because all the *ATG* genes directly required for autophagy and the Cvt pathway are nonessential, and the *loxP–Cre* system allows the use and recycling of markers for MKOs (Fig. 1 A; Gueldener et al., 2002). Among the 31 *ATG* genes, 24 of them were deleted in strain YCY123 (Table I). *ATG15*, *ATG22*, *ATG25*, *ATG26*, *ATG28*, and *ATG30* were not deleted because the first two function after autophagosomes fuse with the lysosomal/vacuolar membrane, and the rest are either not found in *Saccharomyces cerevisiae* or are only required for peroxisome degradation in other methylotrophic yeasts (Cao and Klionsky, 2007). *ATG31* was not deleted because we finished generating the MKO strain and the experiments described in this manuscript before it was published (Kabeya et al., 2007). We refer to strain YCY123 as the MKO strain. Additional deletions or the presence of *ATG* genes are indicated in parentheses.

The MKO strain does not have any obvious unexpected defect other than a slight growth delay (Fig. 1 B). In the MKO strain, we observed one abnormally enlarged vacuole, which is similar to the *atg18Δ* phenotype (Fig. 1 C; Dove et al., 2004). The normal vacuole morphology was restored when we introduced Atg18 back into the MKO strain (Fig. 1 C). We also tested whether the MKO strain was defective for other vacuolar targeting pathways. Carboxypeptidase Y (Prc1) transits through the ER, Golgi complex, and late endosome–multivesicular body (MVB) for delivery to the vacuole. Carboxypeptidase S (Cps1) is a cargo for the MVB pathway and transits through the early secretory pathway similar to Prc1, but is packaged into lumenal vesicles of the MVB before vacuolar delivery. Vacuolar alkaline phosphatase (Pho8) is transported through the ER to the Golgi, but it bypasses the endosome–MVB (Bowers and Stevens, 2005). By pulse-chase analysis and immunoprecipitation, we followed Prc1, Cps1, and Pho8 processing in the MKO strain. As *ATG6* is essential for the carboxypeptidase Y pathway, we transformed a plasmid expressing Atg6 into the MKO and the *atg6Δ* strains. As shown in Fig. 1 D, although there was a kinetic delay in the MKO strain expressing Atg6, most of the precursor Prc1, Cps1 (not depicted), and Pho8 became mature after 45 min in chase medium. Taking the growth delay of the MKO strain into consideration, these data suggest that the MKO strain expressing Atg6 is not defective for the carboxypeptidase Y, MVB, and alkaline phosphatase vacuolar protein delivery pathways, which are nonautophagic.

Components necessary and sufficient for cargo packaging in the Cvt pathway

We next wanted to determine if the MKO strain faithfully reproduced different steps of autophagy when expressing the appropriate autophagy genes. Previous studies with standard deletion strains have only been able to demonstrate the requirement, but not the sufficiency, for various proteins involved in different steps of autophagy. In the next set of experiments, we reconstituted the cargo packaging step of the Cvt pathway. At the beginning of the cargo packaging process, prApe1 forms a large oligomer, and a bright single punctate structure representing the oligomer can be observed by fluorescence microscopy if the protein is tagged with a fluorophore (Kim et al., 1997; Shintani et al., 2002). The same pattern was also detected in the MKO (*atg15Δ RFP-APE1*) strain expressing prApe1 tagged with RFP (Fig. 2 A, left). Additional knockout of *ATG15* in the MKO strain slightly reduced its growth rate but did not affect Cvt vesicle/autophagosome

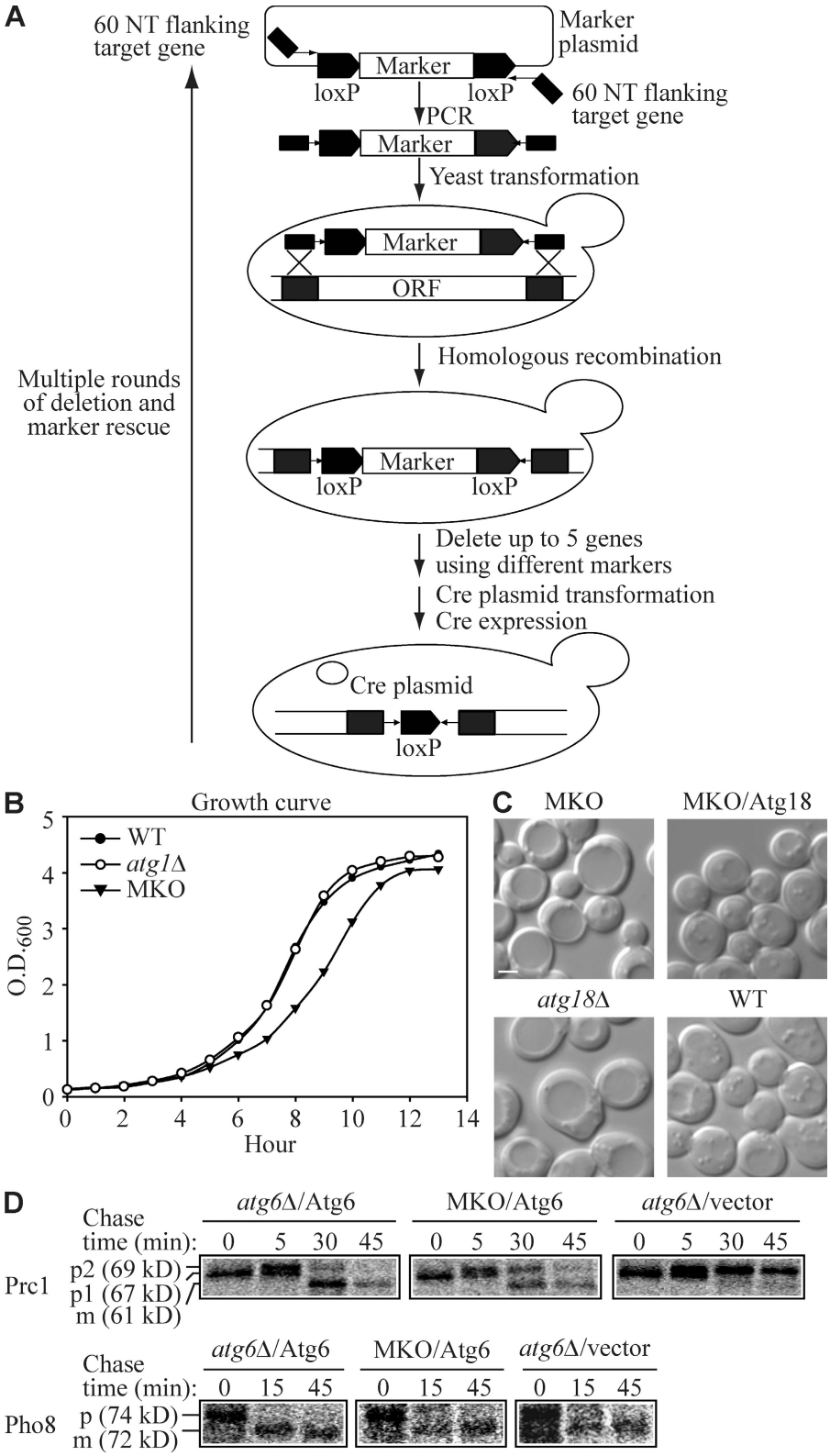

Figure 1. **Generation and properties of the MKO strain.** (A) Schematic representation of the MKO strategy. The *loxP–Cre* system allows disruption of up to five genes using different markers, and efficient removal of markers by Cre expression. Multiple rounds of deletion and marker rescue yielded the MKO strain. See Materials and methods for detailed information. (B) Growth curve of the MKO strain compared with wild-type (WT) and *atg1Δ* strains. WT, *atg1Δ*, and the MKO strains were grown overnight in YPD and diluted to OD_{600} = 0.1. Aliquots were removed for OD_{600} readings every hour for 13 h. (C) Morphology of the MKO strain. WT and *atg18Δ* strains and the MKO strain with or without a plasmid expressing Atg18 (pATG18(415)) were grown in YPD to mid-log phase and observed by microscopy. The MKO strain had an enlarged vacuole similar to the *atg18Δ* strain; once transformed with Atg18, the vacuole size became the same as that in the wild type. Bar, 2 μm. (D) The MKO strain expressing Atg6 is not defective for the carboxypeptidase Y, MVB, or alkaline phosphatase pathways, and was assayed by pulse-chase experiments for Prc1, Cps1 (not depicted), and Pho8 processing. The *atg6Δ* and MKO strains transformed with a plasmid expressing Atg6 (pATG6(414)) or the empty pRS414 vector were subjected to a radioactive label/nonradioactive chase and triple-immunoprecipitated as described in Materials and methods, then analyzed by 8% SDS-PAGE. Carboxypeptidase Y (Prc1) transits through the ER in a precursor (p1) form, acquires its p2 form in the Golgi complex, and, via the late endosome–MVB pathway, is delivered to the vacuole and converted to its mature (m) form. Vacuolar alkaline phosphatase (Pho8) is transported through the ER to the Golgi in a precursor (p) form but bypasses the endosome and is proteolytically activated to its mature (m) form in the vacuole. Atg6 is not required for the alkaline phosphatase pathway; however, for consistency, cells expressing Atg6 were used throughout the experiment.

formation (not depicted). In *ape1Δ* cells, both the Atg19 receptor and the Atg11 adaptor are dispersed in the cytosol (Yorimitsu and Klionsky, 2005). To determine whether the MKO strain reproduced these phenotypes, we constructed a version lacking *APE1* and transformed it with a plasmid expressing either YFP-Atg19 or GFP-Atg11. In the absence of prApe1 (the cargo), YFP-Atg19 was cytosolic (Fig. 2 A, middle), but GFP-Atg11 formed a punctate structure (Fig. 2 A, right). Atg11 is able to interact with itself and several other Atg proteins, and the coiled-coil domains through which Atg11 self-interacts overlap with the interaction sites used by Atg1, Atg17, and Atg20 (Yorimitsu and Klionsky, 2005). Therefore, it is possible that without competition

Table I. **Yeast strains used in this study**

Strain	Descriptive name	Genotype	Source or reference
CWY241	WT (*ATG17-GFP*)	SEY6210 *ATG17-GFP::HIS3*	(Cheong et al., 2005)
HCY107	MKO (*ATG17-GFP*)	YCY123 *ATG17-GFP::HIS3*	This study
HCY113	MKO (*ATG29 ATG17-GFP*)	YCY121 *ATG17-GFP::HIS3*	This study
HCY151	MKO (*ATG11 ATG17-GFP*)	YCY152 *ATG17-GFP::HIS3*	This study
JLY2	*atg12Δ*	SEY6210 *atg12Δ::kanMX*	This study
PSY161	*atg6Δ*	SEY6210 *atg6Δ::HIS3*	This study
SEY6210	WT	*MATα ura3–52 leu2–3,112 his3-Δ200 trp1-Δ901 lys2–801 suc2-Δ9 GAL*	(Robinson et al., 1988)
TVY1	*pep4Δ*	SEY6210 *pep4Δ::LEU2*	(Gerhardt et al., 1998)
WHY001	*atg1Δ*	SEY6210 *atg1Δ::HIS5*	(Shintani et al., 2002)
YCY26	*atg18Δ*	SEY6210 *atg18Δ::kanMX*	This study
YCY32	*atg4Δ atg8Δ*	SEY6210 *atg4Δ::LEU2, atg8Δ::HIS5*	This study
YCY121	MKO (*ATG29*)	SEY6210 *atg1Δ, 2Δ, 3Δ, 4Δ, 5Δ, 6Δ, 7Δ, 8Δ, 9Δ, 10Δ, 11Δ, 12Δ, 13Δ, 14Δ, 16Δ, 17Δ, 18Δ, 19Δ, 20Δ, 21Δ, 23Δ, 24Δ, 27Δ*	This study
YCY123	MKO	SEY6210 *atg1Δ, 2Δ, 3Δ, 4Δ, 5Δ, 6Δ, 7Δ, 8Δ, 9Δ, 10Δ, 11Δ, 12Δ, 13Δ, 14Δ, 16Δ, 17Δ, 18Δ, 19Δ, 20Δ, 21Δ, 23Δ, 24Δ, 27Δ, 29Δ*	This study
YCY124	MKO (*atg15Δ*)	YCY123 *atg15Δ::kanMX*	This study
YCY125	MKO (*atg15Δ ape1Δ*)	YCY123 *atg15Δ::kanMX, ape1Δ::HIS3*	This study
YCY126	MKO (*atg15Δ RFP-APE1*)	YCY123 *atg15Δ::kanMX, RFP-APE1::LEU2*	This study
YCY137	MKO (*ATG3*)	SEY6210 *atg1Δ, 2Δ, 4Δ, 5Δ, 6Δ, 7Δ, 8Δ, 9Δ, 10Δ, 11Δ, 12Δ, 13Δ, 14Δ, 16Δ, 17Δ, 18Δ, 19Δ, 20Δ, 21Δ, 23Δ, 24Δ, 27Δ, 29Δ*	This study
YCY152	MKO (*ATG11*)	YCY123 *ATG11::LYS2*	This study

WT, wild type.

from the other Atg proteins, Atg11 can form a large oligomer by self-interaction in the MKO strain. Analysis of the Atg11 protein by gradient fractionation suggests that it indeed forms a large complex in the MKO strain (unpublished data).

In wild-type cells, Atg19 binds the propeptide of, and colocalizes with, prApe1. Atg11 interacts with Atg19 and targets the complex to the PAS (Scott et al., 2001; Shintani et al., 2002; Yorimitsu and Klionsky, 2005). Thus, there is a temporal order of protein interaction, whereby Atg11 cannot bind the prApe1 complex in the absence of Atg19. To test whether this temporal organization is faithfully retained in the MKO strain, we transformed the MKO (*atg15Δ RFP-APE1*) strain with plasmids expressing YFP-Atg19, CFP-Atg11, or both. In agreement with the previous model, RFP-Ape1 and YFP-Atg19 colocalized with each other in the absence of other Atg proteins (Fig. 2 B, top). In contrast, without Atg19, RFP-Ape1 did not colocalize with CFP-Atg11 (Fig. 2 B, middle). The three proteins colocalized in a single punctum when all of them were coexpressed (Fig. 2 B, bottom). These data suggest that prApe1, Atg19, and Atg11 are necessary and sufficient for cargo packaging in the Cvt pathway. We note, however, that only ∼50% of the puncta representing the cargo complex (comprised of prApe1, Atg19, and Atg11) were at the PAS (i.e., perivacuolar), which suggests that additional Atg proteins are required to facilitate the targeting of the cargo complex to this site.

Assembly of the initial starvation-specific PAS

The analysis of cargo packaging verified that the MKO strain faithfully replicated the temporal order of Atg protein interactions that have been deduced from previous studies. Next, we decided to use the MKO strain to address a question that would otherwise be extremely difficult to approach. In particular, we wanted to determine the order of assembly of Atg proteins at the PAS. In theory, it might be possible to order the proteins through an extensive analysis of multiple deletion strains, generating a series of epistatic relationships. However, a definitive study is best performed in the complete absence of the other (i.e., those not being examined) Atg proteins. Recent studies suggest that Atg11 and Atg17 are the two initial factors that establish the assembly sequence for Atg proteins at the PAS (Shintani et al., 2002; Suzuki et al., 2007). In particular, Atg11 is critical for PAS assembly during vegetative growth, whereas Atg17 is proposed to act as a scaffold for recruiting other Atg proteins during starvation-specific PAS formation.

To test whether Atg17 itself is sufficient to assemble the initial PAS, we observed the localization of Atg17 tagged with GFP in the MKO strain by fluorescence microscopy. In wild-type cells, Atg17-GFP displayed a clear PAS punctum as well as a diffuse cytosolic signal in both vegetative and starvation conditions; in some cells, we could detect more than one punctum, particularly under starvation conditions (Fig. 3 A). In contrast, Atg17-GFP was largely cytosolic in the MKO (*ATG17-GFP*) strain (Fig. 3 A, vector), which suggests that Atg17 is not sufficient for the initial PAS assembly even during starvation. Therefore, we decided to determine what additional factors were needed to allow correct localization of Atg17 during autophagy.

Recently, it was found that Atg1 and Atg13 are required along with Atg17 in assembly of the starvation-specific PAS

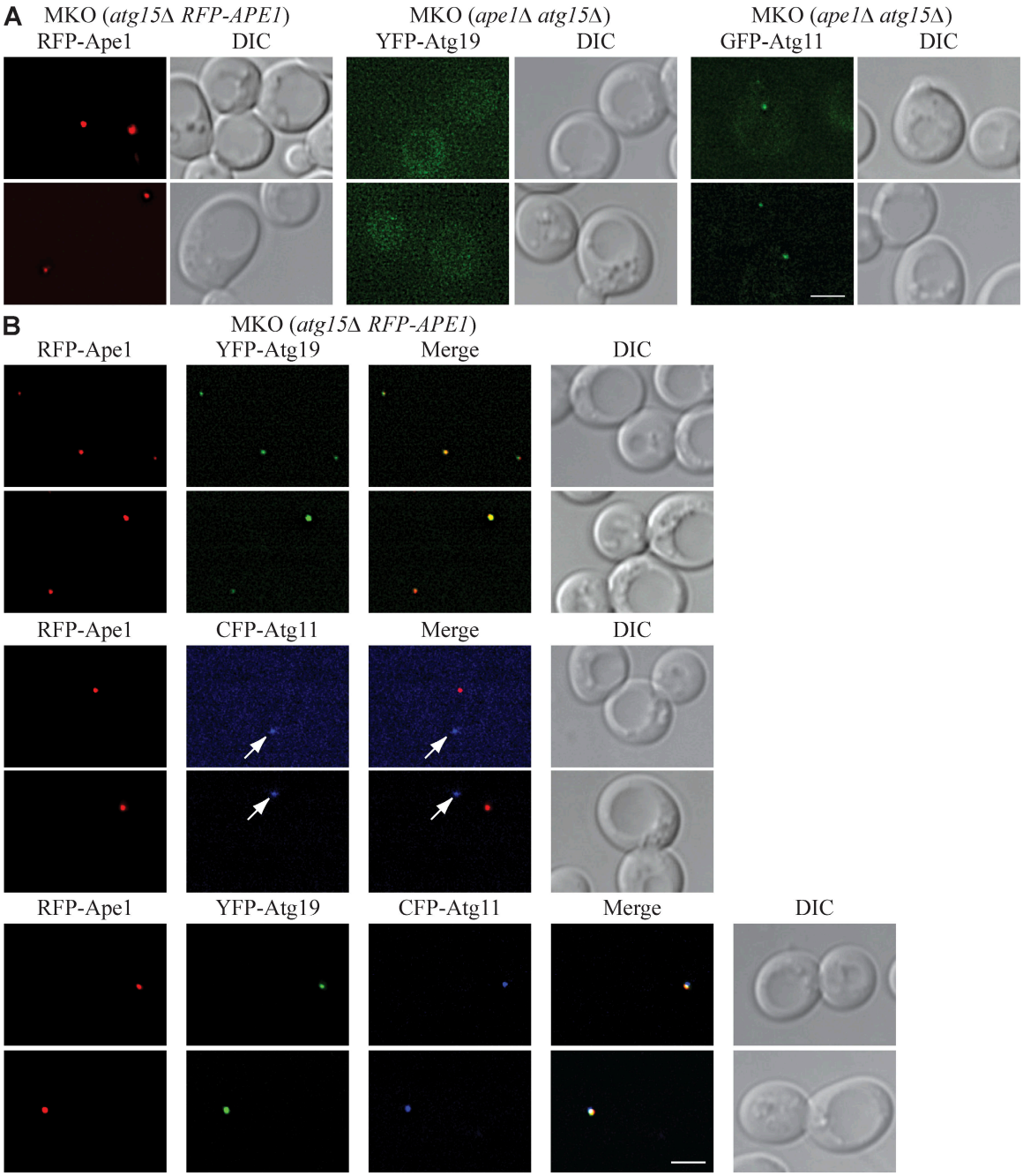

Figure 2. **Reconstitution of the cargo recognition and packaging step of the Cvt pathway.** (A) Localization of the cargo prApe1 in the MKO (*atg15Δ RFP-APE1*) strain, and localization of the receptor Atg19 and the adaptor Atg11 in the MKO (*ape1Δ atg15Δ*) strain. The MKO (*atg15Δ RFP-APE1*) strain and the MKO (*ape1Δ atg15Δ*) strain transformed with a plasmid expressing YFP-Atg19 (pYFPATG19(416)) or HA-tagged CFP-Atg11 (pCuHACFPATG11(414)) were grown in selective SMD medium to mid-log phase and observed by fluorescence microscopy. DIC, differential interference contrast. (B) Colocalization of prApe1, Atg19, and Atg11. The MKO (*atg15Δ RFP-APE1*) strain was transformed with a plasmid expressing YFP-Atg19, HA-tagged CFP-Atg11, or both, grown to mid-log phase and observed by fluorescence microscopy. When Atg19 was coexpressed with prApe1 in the MKO (*atg15Δ RFP-APE1*) strain, the cargo prApe1 colocalized with the receptor Atg19 (top). When Atg19 was absent, the adaptor Atg11 (arrows) did not colocalize with the cargo (middle). When prApe1, Atg19, and Atg11 were all present, the three proteins colocalized to the same structure (bottom). Bars, 2.5 μm.

(Cheong et al., 2008). Accordingly, we hypothesized that Atg1, Atg13, and Atg17 are all required for the initial PAS assembly during nonspecific autophagy. To examine this, we transformed plasmids expressing Atg1, Atg13, or both into the MKO (*ATG17-GFP*) strain and observed localization of Atg17-GFP by fluorescence microscopy. Atg17-GFP showed clear punctate structures under starvation conditions only when Atg1 and Atg13 were expressed together (Fig. 3 A, Atg1 + Atg13). In contrast, expression of either Atg1 or Atg13 alone or in combination with Atg11 did not facilitate Atg17-GFP puncta formation (Fig. 3 A). The same localization pattern was detected with GFP-Atg1; this protein was cytosolic when expressed by itself, and formed punctate structures in starvation conditions only when Atg13 and Atg17 were both present (unpublished data). Furthermore,

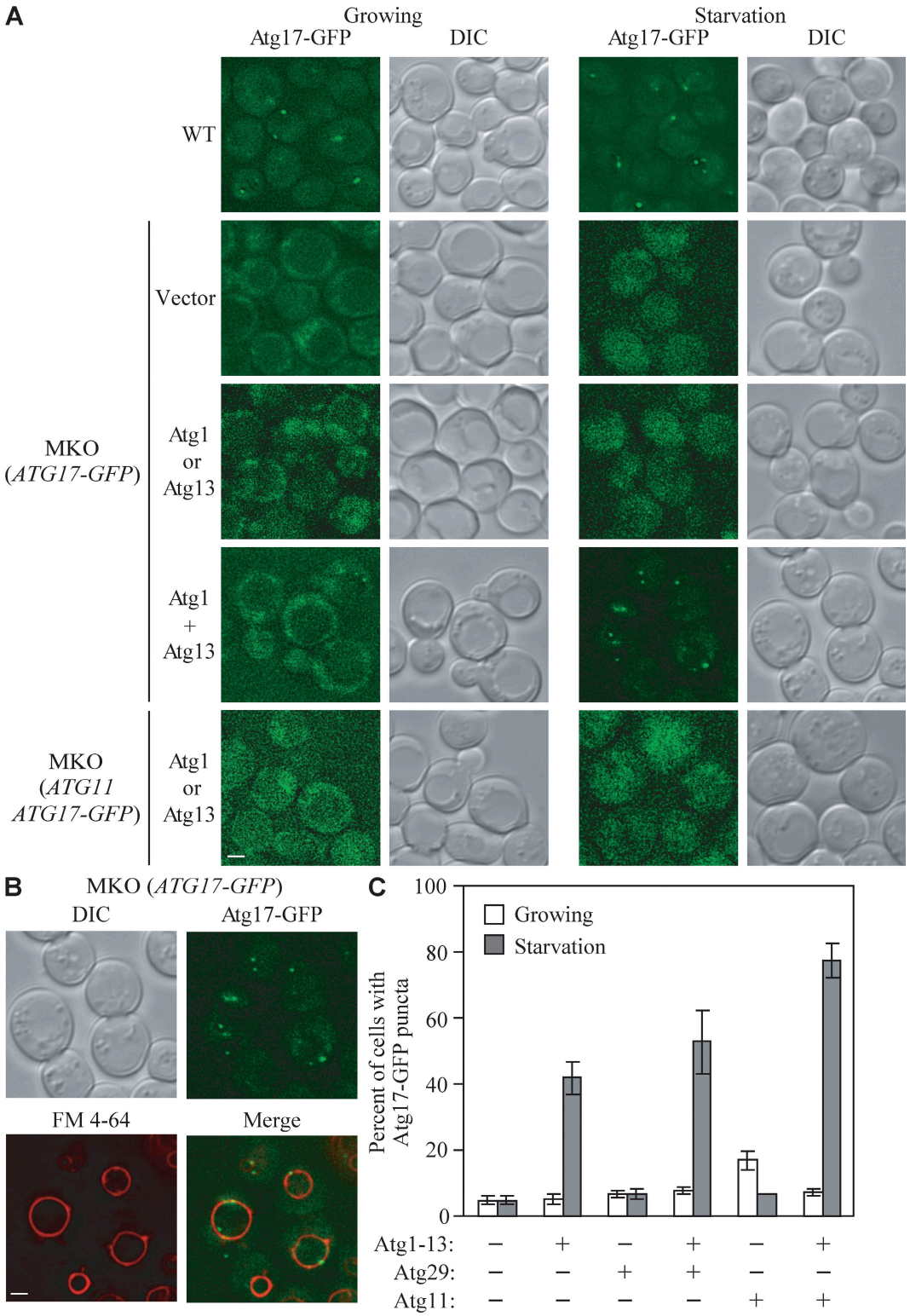

Figure 3. **Reconstitution of the initial step of starvation-specific PAS assembly.** (A) Localization of Atg17-GFP in the wild-type (WT) and MKO (*ATG17-GFP*) strains. The WT (*ATG17-GFP*) strain; the MKO (*ATG17-GFP*) strain transformed with vector (pRS415), a plasmid expressing Atg1 (pATG1(415)), Atg13 (pATG13(415)), or both Atg1 and Atg13 (pATG1-ATG13(415)); and the MKO (*ATG11 ATG17-GFP*) strain transformed with a plasmid expressing Atg1 or Atg13 were grown in selective SMD medium to mid-log phase and shifted to SD-N for 2 h for starvation. Samples were taken from both growing (mid-log phase) and starvation conditions for fluorescence microscopy analyses. Atg17-GFP displayed a punctate structure in WT cells in both growing and starvation conditions; some cells had more than one punctum in starvation conditions. In the MKO (*ATG17-GFP*) strain, Atg17 was cytosolic in both conditions; its localization pattern changed to punctate structures in starvation only when Atg1 and Atg13 were coexpressed. Coexpression of Atg1 and Atg11 or Atg13 and Atg11 could not redistribute Atg17 from the cytosol to punctate structures. Representative images are shown. DIC, differential interference contrast. (B) Perivacuolar localization of Atg17-GFP in the MKO (*ATG17-GFP*) strain. The MKO (*ATG17-GFP*) strain transformed with a plasmid expressing both Atg1 and Atg13 (pATG1-ATG13(415)) was grown to mid-log phase, stained with the vacuolar dye FM 4–64 as described in Materials and methods, and shifted

~75% of Atg17-GFP or GFP-Atg1 puncta were perivacuolar (detected with the lipophilic dye FM 4-64), which indicates that Atg1, Atg13, and Atg17 are sufficient for the initial PAS assembly during starvation (Fig. 3 B). All together, these data suggest that Atg17 is not sufficient for starvation-specific PAS formation; rather, Atg1, Atg13, and Atg17 all appear to have an initial role in PAS assembly during starvation.

Finally, we quantified the percentage of cells containing Atg17-GFP puncta in the MKO strain expressing different Atg proteins. Approximately 40% of the cells coexpressing Atg1 and Atg13 showed Atg17-GFP puncta under starvation conditions, whereas <5% of the cells displayed any punctate structure when Atg17-GFP was expressed by itself (Fig. 3 C). Additional expression of other components in the Atg17 complex further increased the percentage of cells displaying Atg17-GFP puncta. For example, Atg29 by itself did not significantly affect Atg17-GFP puncta formation, but expression of Atg29 in the presence of Atg1 and Atg13 increased the percentage of cells with puncta to ~53% during starvation. Atg11, when expressed together with Atg1 and Atg13, resulted in an even greater increase to ~80% (Fig. 3 C). Collectively, these results indicate that starvation-specific PAS formation initially requires a minimal set of Atg proteins consisting of Atg1, Atg13, and Atg17; other components in the Atg1 complex, such as Atg29 and Atg11, further enhance assembly.

The Atg8 conjugation system affects formation of the Atg12–Atg5 conjugate

Having established that the MKO strain reproduces the temporal order of action of components involved in cargo packaging in growing conditions, and determined the initial factors for PAS assembly during starvation, we decided to extend our analysis of the utility of this system. In particular, we chose to examine the Atg12–Atg5 conjugation system because this part of the autophagy process has been reconstituted in vitro. Therefore, components have been identified that are both necessary and sufficient for the reaction. The question we posed was whether the information gained from these previous experiments accurately reflected the complete in vivo situation. Previous data show that Atg5, Atg7, Atg10, and Atg12 are essential for the conjugation (Mizushima et al., 1998), and Atg16 is required for the efficiency of this reaction (Mizushima et al., 1999), but Atg3, Atg4, and Atg8 from the Atg8–PE system are not involved in Atg12–Atg5 conjugation (Kuma et al., 2002). Accordingly, we expressed various combinations of these proteins in the MKO strain. We used 3× HA-tagged Atg12 to allow detection of the Atg12–Atg5 conjugate. When expressed in an *atg12Δ* strain, we detected both free HA-Atg12 and HA-Atg12 conjugated to Atg5 (Fig. 4, lane 2). As expected, when only Atg5 and HA-Atg12 were expressed in the MKO strain, we did not detect the conjugated species (Fig. 4, lane 4). In contrast, if Atg7 and Atg10 were also present, we detected a faint band corresponding to the HA-Atg12–Atg5 conjugate; however, the majority of the HA-Atg12 was in the free form (Fig. 4, lane 5). When we added Atg16, we found that a substantially greater amount of conjugate was formed (Fig. 4, lane 6).

Next, we examined possible contributions from the Atg8 conjugation system. When we expressed Atg4 and Atg8 together with Atg5, Atg7, Atg10, Atg12, and Atg16, the Atg12–Atg5 conjugation efficiency was further enhanced (Fig. 4, lane 7). Atg8–PE was not generated in this strain because of the absence of Atg3 (not depicted). Thus, it seems that even without the formation of Atg8–PE, the presence of some proteins in the Atg8–PE system can facilitate the conjugation of Atg12 to Atg5. Furthermore, the level of the Atg12–Atg5 conjugate was even greater when Atg3 was added (Fig. 4, lane 8). Thus, our data suggest that Atg5, Atg7, Atg10, and Atg12 are minimum requirements for Atg12–Atg5 conjugate formation, and Atg16 facilitates the conjugation, in agreement with published data. We further found, however, that components in the Atg8–PE system also enhance the conjugation reaction. The same conclusions were reached in either vegetative (Fig. 4) or starvation (not depicted) conditions.

Atg8–PE formation and Atg4 cleavage

We extended our analysis with the MKO strain to the reconstitution of Atg8–PE conjugation. Although there have been extensive studies on the in vitro reconstitution of Atg8–PE, in vivo reconstitution has only been described in *Escherichia coli* where autophagy does not occur (Ichimura et al., 2004). The C-terminal arginine of nascent Atg8 is normally removed by Atg4, which can also release Atg8 from PE. When the C-terminal arginine is removed, as in Atg8ΔR, the initial processing step is bypassed. Previous experiments using purified Atg8ΔR, Atg3, Atg7, and PE-containing liposomes suggest that Atg8–PE formation is at its peak when the PE content reaches 70% of the total membrane, but with a concentration close to that of yeast organelle membranes, the efficiency is very low (Ichimura et al., 2004). However, the efficiency of conjugation is boosted by the presence of the Atg12–Atg5 conjugate, and further addition of Atg16 only slightly increases Atg8–PE formation (Hanada et al., 2007). Our data support this current view of Atg8 lipidation. Moreover, they provided additional insights into both the conjugation and deconjugation reactions.

We first tested if Atg8, Atg4, Atg7, and Atg3 are sufficient for Atg8–PE formation. When we transformed a plasmid expressing these proteins into the MKO (*ATG3*) strain, Atg8–PE was essentially not detected in both growing and starvation conditions (Fig. 5 A, lane 3); even when we expressed all the components for the Atg12–Atg5 conjugation system, we were still not able to detect a signal for Atg8–PE (Fig. 5 A, lane 4). These data do not agree with the in vitro reconstitution data. One of the

to SD-N for 2 h before imaging. When both Atg1 and Atg13 were expressed, Atg17-GFP puncta localized at perivacuolar sites under starvation conditions. Bars, 2.5 μm. (C) The number of cells that contained Atg17-GFP PAS puncta in MKO strains (HCY107, HCY113, and HCY151) with coexpression of various combinations of Atg proteins was quantified under vegetative (open bars) and starvation (closed bars) conditions. Approximately 100–250 cells for each strain were analyzed for scoring the percentage of cells with fluorescent PAS puncta.

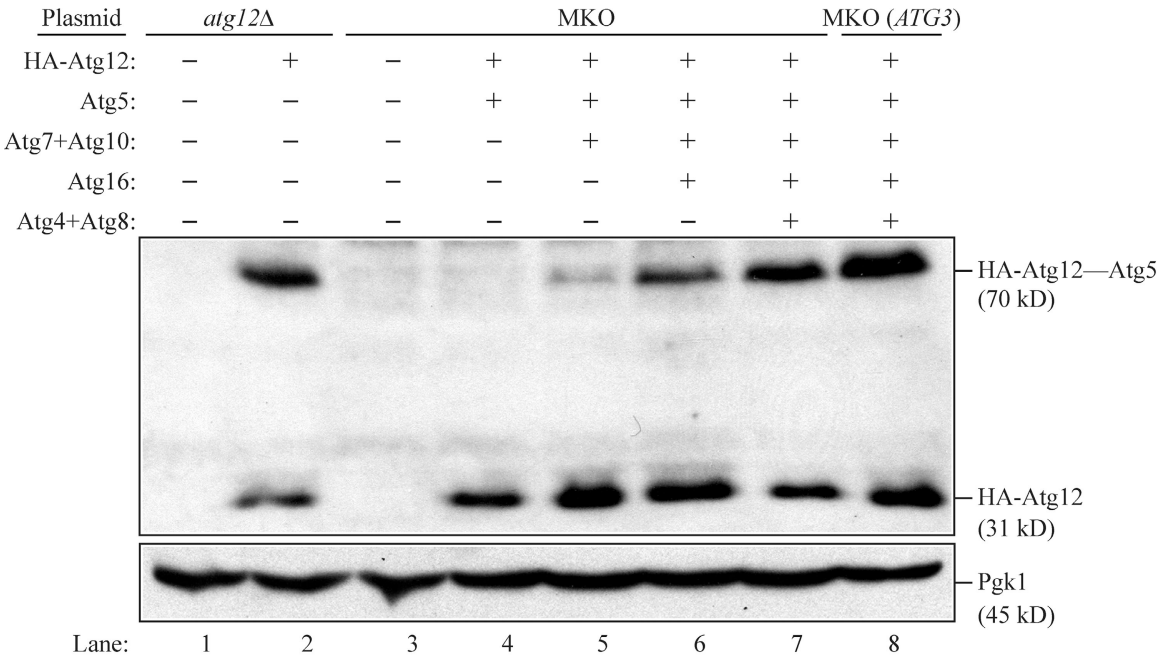

Figure 4. **Reconstitution of the Atg12–Atg5 conjugation system.** MKO, MKO (*ATG3*), and *atg12Δ* cells transformed with various plasmids were grown in selective SMD medium, collected at mid-log phase, and subjected to Western blot analysis using an anti-HA antibody. 0.2 OD_{600} units of cells were loaded in each lane. Pgk1 was used as a loading control. Plasmids expressing HA-tagged Atg12 (pHA-ATG12(416)); Atg7 and Atg10 (pATG7-ATG10(414)); Atg5 and HA-tagged Atg12 (pATG5-HA-ATG12(416)); Atg5, HA-Atg12, and Atg16 (pATG5-HA-ATG12-ATG16(416)); and Atg8, Atg4, Atg7, and Atg10 (pATG8-ATG4-ATG7-ATG10(414)) were used as indicated. With Atg5, Atg12, Atg7, and Atg10 expressed in the MKO strain, a small amount of Atg12–Atg5 conjugate formed (lane 5). Additional expression of Atg16 improved the conjugation efficiency (lane 6). The presence of Atg8, Atg4, and Atg3 from the Atg8 conjugation system further facilitated the formation and/or enhanced the stability of Atg12–Atg5 (lanes 7 and 8).

differences between these previous studies and our experiments is that the previous analyses used the modified Atg8ΔR to bypass the need for the initial Atg4 cleavage, and omitted Atg4 from the subsequent reactions. However, the absence of Atg4 also blocks the deconjugation of Atg8–PE and thus favors the accumulation of the conjugated species. Considering the role of Atg4 in determining the balance between Atg8 and Atg8–PE, we introduced a plasmid expressing Atg8ΔR, Atg7, and Atg10, into the MKO (*ATG3*) strain; in this case, a significant amount of Atg8–PE was detected (Fig. 5 A, lane 5). When we additionally expressed Atg5, HA-Atg12, and Atg16, almost all of the Atg8 was in its conjugated form (Fig. 5 A, lane 6). Thus, when Atg4 is present, as is the case in vivo, Atg8–PE levels are extremely low in the MKO strain, even in the presence of the Atg12–Atg5 conjugation system. These results suggest that the in vitro system does not faithfully reflect the contribution of other factors that are required to control the activity of Atg4.

Finally, we attempted to further define the reason for the low level of Atg8–PE in this system. In wild-type cells, a population of Atg8 is constantly degraded inside the vacuole, so the total amount of Atg8 is lower than that in the MKO strain. Therefore, we used a *pep4Δ* strain, which blocks Atg8 degradation, as a control (Fig. 5 B, lane 11). When deconjugation occurs, an Atg8–PE band was not detected (Fig. 5 B, lane 3), whereas expression of Atg8ΔR in an *atg4Δ atg8Δ* strain defective in deconjugation causes all of the protein to accumulate in the lipidated form (Fig. 5 B, lane 10). When we expressed Atg8ΔR, Atg7, and Atg10 along with Atg5, Atg12, or Atg16 separately, Atg8–PE conjugation was not increased (Fig. 5 B, lane 4–7). However, the presence of the Atg12–Atg5 conjugate facilitated Atg8–PE formation (Fig. 5 B, lane 8; and not depicted). In this in vivo system, Atg16 also facilitated the formation and/or enhanced the stability of Atg8–PE (Fig. 5 B, lane 9), which could be indirect through its action on the Atg12–Atg5 conjugate (Fig. 4, lane 6).

Discussion

In this study, we created and validated an MKO strain in which 24 *ATG* genes directly required for autophagy and the Cvt pathway were deleted (Fig. 1). Using this in vivo system, we determined minimum requirements for cargo packaging (Fig. 2), initial starvation-specific PAS assembly (Fig. 3), Atg12–Atg5 conjugation (Fig. 4), and Atg8–PE formation (Fig. 5). Although single- and double-deletion analyses and in vitro reconstitution have provided us with important insights into mechanisms, in general the minimum requirements for, and regulation of, these steps have not been explored extensively. The MKO strain serves as a valuable and powerful tool for these purposes. Moreover, it also has an obvious advantage over an in vitro reconstitution system, more accurately recapitulating what occurs in vivo and making studies of complex steps/aspects of autophagy possible and more efficient.

Our in vivo reconstitution of the Atg12–Atg5 and Atg8–PE conjugation systems demonstrated the usefulness of the MKO strain, as it provided us with information missing from the in vitro studies. For example, our data suggest that components in the Atg8–PE system contribute to the efficiency of Atg12–Atg5

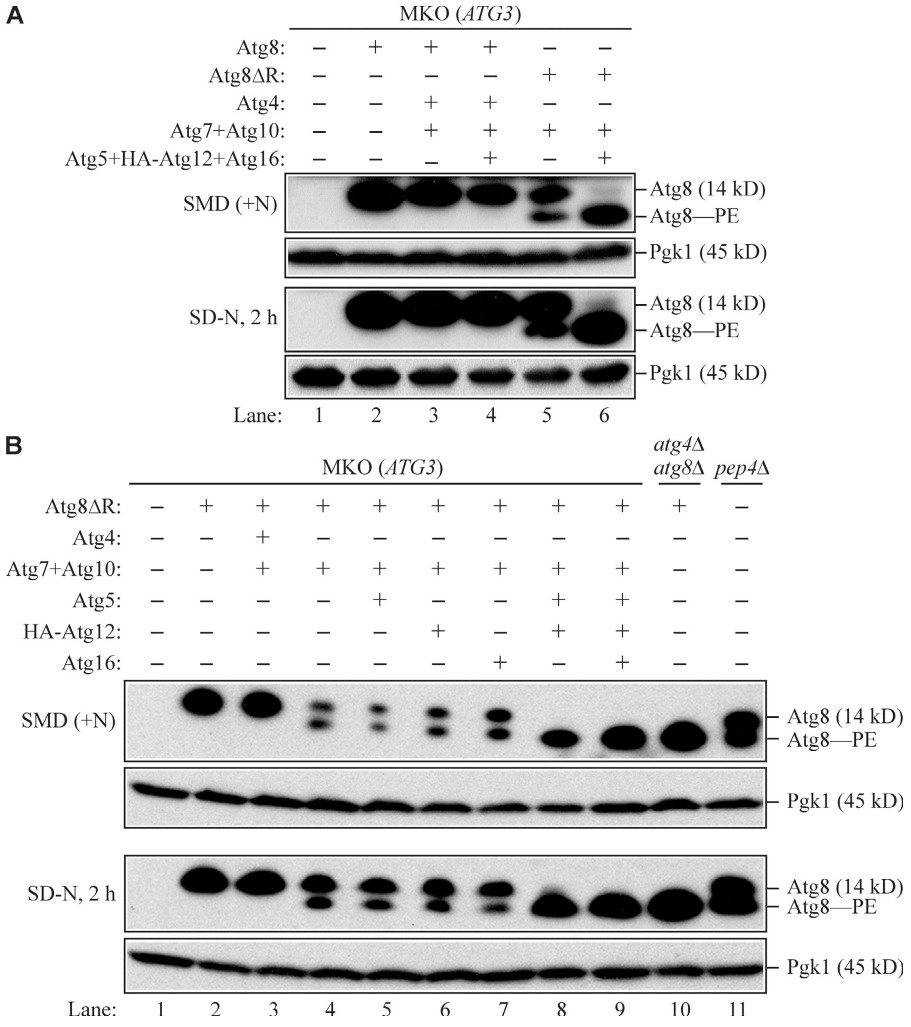

Figure 5. **Reconstitution of the Atg8–PE conjugation system.** (A) The role of Atg4 and the Atg12–Atg5 conjugation system in Atg8–PE formation. MKO (*ATG3*) cells transformed with different combinations of plasmids were grown in selective SMD medium, collected at mid-log phase or 2 h after starvation, and then subjected to Western blot analysis using anti-Atg8 antiserum. 0.2 OD_{600} units of cells were loaded in each lane. Pgk1 was used as a loading control. Plasmids expressing Atg8 (pATG8(414)); Atg8, Atg4, Atg7, and Atg10 (pATG8-ATG4-ATG7-ATG10(414)); Atg5, HA-Atg12, and Atg16 (pATG5-HA-ATG12-ATG16(416)); and Atg8ΔR, Atg7, and Atg10 (pATG8ΔR-ATG7-ATG10(414)) were used as indicated. Atg8–PE was hardly detected in both growing and starvation conditions even when all the known components from the Atg8–PE and Atg12–Atg5 conjugation systems were expressed (lane 4). However, when Atg8ΔR was expressed and Atg4 was absent, a significant amount of Atg8–PE was observed (lane 5), and the amount was further increased when all the components from the Atg12–Atg5 conjugation system were also expressed (lane 6). Note that Atg8–PE migrates aberrantly during SDS-PAGE and runs lower than Atg8. (B) The role of the Atg12–Atg5 conjugation system on Atg8–PE formation. The experimental procedures were the same as in A. Plasmids expressing Atg8ΔR (pATG8ΔR(414)); Atg8ΔR, Atg4, Atg7, and Atg10 (pATG8ΔR-ATG4-ATG7-ATG10(414)); Atg8ΔR, Atg7, and Atg10; Atg5 (pATG5(416)); HA-tagged Atg12 (pHA-ATG12(416)); Atg16 (pATG16(416)); Atg5 and HA-Atg12 (pATG5-HA-ATG12(416)); and Atg5, HA-Atg12, and Atg16 were used as indicated. The *atg4Δ atg8Δ* strain transformed with the plasmid expressing Atg8ΔR (pATG8ΔR(414)) and the *pep4Δ* strain were used as controls (lanes 10 and 11). When Atg4 was present, an Atg8–PE band was not detected (compare lanes 3 and 4). Expression of Atg5, Atg12, or Atg16 alone did not improve Atg8–PE formation (compare lanes 5–7 to lane 4). When the Atg12–Atg5 conjugate was formed through the expression of Atg7, Atg10, Atg12, and Atg5, the efficiency of Atg8–PE formation was greatly enhanced (lane 8). Atg16 further facilitated Atg8–PE conjugation and/or enhanced the stability of the conjugate (lane 9).

conjugation (Fig. 4). With regard to the Atg8–PE conjugation system, the results are even more intriguing. We find that when Atg4 is present to cleave the C-terminal arginine of Atg8 and to deconjugate Atg8 from PE, a situation that is more physiologically relevant than the conditions used for the in vitro reconstitution studies; even all the proteins in the two conjugation systems cannot sustain a detectable amount of Atg8–PE (Fig. 5 A), in contrast to wild-type cells. This means that either deconjugation occurs too quickly, conjugation efficiency is still somehow compromised in the MKO strain, or both. One possibility is that the plasmid-based Atg4 in the MKO strain results in overexpression and elevated Atg4 activity that favors deconjugation of Atg8–PE. Because we do not have antibodies against the Atg4 protein, we cannot directly determine the Atg4 levels. To address this possibility, however, we examined the functionality of our Atg4-expressing plasmid in an *atg4Δ* strain. We found that expression of Atg4 in the *atg4Δ* strain complemented prApe1 maturation, and this strain did not accumulate unconjugated Atg8 (unpublished data), which suggests that our plasmid expressing Atg4 is functional, and that additional factors are needed to regulate Atg4's protease activity or deconjugation function in the MKO strain. Regulation of Atg4 is an important topic for autophagy. For example, why is Atg8 synthesized with residues after the C-terminal glycine when these residues are immediately removed by Atg4? Also, how is Atg4 regulated to prevent premature deconjugation of Atg8–PE? One recent study suggests that Atg4 activity is subject to redox regulation (Scherz-Shouval et al., 2007), although the actual mechanism through which this might occur in vivo is not known. Follow-up analyses will yield more insights into the regulation of deconjugation and conjugation.

With the MKO strain, we can study the order of protein assembly at the PAS more directly and efficiently compared with analyses with single- or double-deletion strains. Previous studies suggest that Atg11 and Atg17 are the initial factors for PAS assembly in vegetative and starvation conditions, respectively (Shintani et al., 2002; Suzuki et al., 2007). However, it is possible that some proteins in the autophagy pathway may act together or be able to substitute for one another in order to target Atg11 and Atg17 to the PAS. Our data suggest that in vegetative

conditions, Atg11 is not sufficient to localize itself and the cargo complex to the PAS even though the cargo complex forms, which means that an additional protein is needed for efficient assembly of the Cvt-specific PAS. We also provided direct evidence that not only Atg17 but also Atg1 and Atg13 are important for the initial starvation-specific PAS assembly (Fig. 3 A). Approximately 75% of the Atg17-GFP puncta observed in the presence of Atg1 and Atg13 were perivacuolar (Fig. 3 B), which suggests that these three proteins are sufficient for this process. We also noted that MKO cells expressing Atg1, Atg13, and Atg17-GFP tend to have more punctate structures than the wild-type cells. Some of the puncta might be precursor or intermediate structures of the initial PAS. In addition to Atg1, Atg13, and Atg17, other proteins such as Atg29 and Atg11 also contribute to the efficiency of the assembly process (Fig. 3 C). During the course of our studies, a paper was published verifying a role for Atg29 in the assembly of the starvation-specific PAS (Kawamata et al., 2008). However, there are some discrepancies between the two sets of studies. For example, Kawamata et al. (2008) found that Atg29 is essential for assembly of the starvation-specific PAS, whereas our present studies indicate that this protein enhances PAS assembly but is not essential. Further analyses will be needed to resolve this and other questions pertaining to this topic. Although Atg11 is a Cvt-specific factor, it contributed to PAS assembly along with Atg1, Atg13, and Atg17 during starvation conditions (Fig. 3 C). Generation of the Cvt-specific PAS that is dependent on Atg11 during vegetative growth may help to recruit components in the Atg17 complex, resulting in enhanced PAS assembly when cells are subsequently shifted to starvation conditions (Cheong et al., 2008).

In vitro systems can be extremely useful and powerful tools for dissecting molecular mechanisms, and the present study does not suggest otherwise. Rather, we demonstrate that in vivo reconstitution can complement and extend in vitro analyses. Generation of a strain with 24 *ATG* genes knocked out is a unique and novel approach for studying complex pathways such as autophagy, and the strain will be a very useful tool for autophagy research. We can foresee potential uses of the strain in determining the temporal order of protein arrival at the PAS, in Atg protein retrieval after autophagosome formation, and many other aspects of autophagy. These experiments will reward us with new findings and open up areas for potential research.

Materials and methods

Yeast strains, media, reagents, and antisera

The yeast *S. cerevisiae* strains used in this study are listed in Table I. Knockout strains were constructed using the *loxP–Cre* system (Gueldener et al., 2002). GFP tagging of Atg17 at the corresponding chromosomal locus was performed by a PCR-based procedure (Longtine et al., 1998). Yeast media including YPD (1% yeast extract, 2% peptone, and 2% dextrose) or synthetic minimal medium with casamino acids (SMD + CA) and SD-N for nitrogen starvation have been described previously (Shintani et al., 2002). FM 4-64 and antibodies to alkaline phosphatase (Pho8) and carboxypeptidase Y (Prc1) were obtained from Invitrogen. Antisera against Ape1 (Klionsky et al., 1992) and Atg8 (Huang et al., 2000) have been described previously. Antibody to the hemagglutinin epitope was obtained from Santa Cruz Biotechnology, Inc. Antisera against Cps1 and phosphoglycerate kinase (Pgk1) were gifts from S. Emr (Cornell University, Ithaca, NY) and J. Thorner (University of California, Berkeley, Berkeley, CA), respectively.

Construction of the MKO strain

The MKO strains were derived from wild-type haploid strain SEY6210 (Robinson et al., 1988), and the *loxP–Cre* system (Gueldener et al., 2002) was modified for multiple gene knockouts (Fig. 1 A). The gene disruption cassette consisting of a selection marker flanked by two *loxP* sequences was amplified by PCR using primers containing 60 nucleotide stretches that are homologous to sequences upstream of the start codon or downstream of the stop codon of the target gene, followed by 19 or 22 nucleotides complementary to sequences flanking the *loxP* sites in the marker plasmid. The PCR products were transformed into yeast cells, and transformants were selected on plates lacking a particular amino acid or containing a specific antibiotic. Selected transformants were checked for correct integration by colony PCR using two sets of primers. *ATG* genes were deleted one at a time using markers including *kanMX*, *ble*^{r}, *HIS5*, *URA3*, and *LEU2*. A maximum of five *ATG* genes were deleted before Cre recombinase was expressed to loop out the markers. Replica plating was used to identify colonies that had lost all of the markers. The markers can thus be reused to delete other *ATG* genes. After several rounds of deletion and marker rescue, 24 *ATG* genes were deleted. The strain was named YCY123 (MKO).

Plasmid construction

For pATG4(414), pATG7(414), pATG10(414), pATG5(416), and pATG16(416), the individual gene with its endogenous promoter and terminator region was amplified from wild-type genomic DNA, digested with SacI, XmaI, KpnI, BamHI, and NotI, respectively, and cloned into the corresponding site of pRS414 or pRS416 (Sikorski and Hieter, 1989). SacI and BamHI sites were used to clone pATG6(414), NotI and NcoI for pATG8(414), SacI and PstI for pATG1(415), and XbaI and XmaI for pATG13(415). For pHA-ATG12(416), the insert was amplified from 3× HA-APG12 (Mizushima et al., 1998) and cloned into pRS416. The functionality of these plasmids was tested in the corresponding knockout strains by examining prApe1 maturation.

The promoter, open reading frame, and terminator inserts were subsequently removed by restriction digestion and cloned in various combinations to generate the multigene plasmids pATG1-ATG13(415), pATG7-ATG10(414), pATG5-HA-ATG12(416), pATG5-HA-ATG12-ATG16(416), and pATG8-ATG4-ATG7-ATG10(414). The key in the design was that the sites for cloning each subsequent gene were not present within the existing plasmid. A one-step site-directed mutagenesis protocol (Zheng et al., 2004) was used to remove the last arginine from the *ATG8* open reading frame to generate pATG8ΔR(414). The NotI- and NcoI-digested Atg8ΔR fragment was exchanged with the Atg8 fragment to generate pATG8ΔR-ATG4-ATG7-ATG10(414), from which Atg4 was removed by BglII and SacII digestion followed by blunt-ending and religation to form pATG8ΔR-ATG7-ATG10(414). Plasmids pRFPAPE1(305) (Stromhaug et al., 2004), pGFPATG11(416) (pGFP-CVT9(416); Kim et al., 2001), pYFPATG19(416) (pYFP-Cvt19; Shintani et al., 2002), pCuHACFPATG11(414) (Yorimitsu and Klionsky, 2005), and pATG18(415) (pCVT18(415); Guan et al., 2001) have been described previously.

Pulse-chase analysis and immunoprecipitation

5 ml of cells in mid-log phase grown in SMD + CA medium were collected and labeled in 500 µl SMD with 20 µCi ^{35}S for 5 min at 30°C. Chase medium (5 ml YPD containing 2 mM cysteine and 1 mM methionine) was added, and at each time point, 1 ml of cells were collected, precipitated with TCA, washed with acetone, dried, and resuspended in 100 µl MURB (50 mM sodium phosphate, 25 mM MES, pH 7.0, 1% SDS, 3 M urea, and 0.5% β-mercaptoethanol). Glass beads were added to break the cells, and then each sample was boiled and diluted in 800 µl TWIP (0.5% Tween 20, 50 mM Tris hydrochloride, pH 7.5, 150 mM NaC1, and 0.1 mM EDTA). The supernatant fraction was subjected to triple immunoprecipitation: the first precipitation was performed with 3 µl Prc1 antiserum, and the supernatant after removal of the antibody–antigen complex with protein A–Sepharose was immunoprecipitated with 1 µl Cps1 antiserum, and then with 6 µl Pho8 antiserum; the second and third immunoprecipitations were performed twice each to eliminate carryover of the previous antisera.

Protein extraction and Western blotting

Yeast cells were grown at 30°C to mid-log phase in the appropriate medium, harvested, resuspended with 10% TCA, and held for 30 min on ice. Cell pellets were washed with 100% acetone, air-dried, and resuspended in MURB buffer. Cells were further broken by vortexing with glass beads and then heated at 75°C for 10 min. For each sample, 0.2 OD_{600} units of

cells were resolved by SDS-PAGE, transferred to a polyvinylidene fluoride membrane, and probed with appropriate antisera or antibodies.

Fluorescence microscopy

Yeast cells were grown to mid-log phase in selective SMD medium. To label the vacuolar membrane, cells were stained with 0.8 mM FM 4-64 for 15 min, washed, and incubated in the same medium for 30 min. For starvation, cells were shifted to SD-N medium for 2 h. 1 ml of cells were pelleted and resuspended in 30 µl of the same medium before imaging. Microscopy was performed at room temperature on a microscope (IX71; Olympus) with a 100× Universal Plan Apochromat objective lens (Olympus) and a camera (CoolSnap HQ; Photometrics). The microscope was controlled by a workstation (DeltaVision Spectris; Applied Precision, LLC). Images were acquired and deconvolved with DeltaVision softWoRx software (Applied Precision, LLC).

This work was supported by National Institutes of Health Public Health Service grant GM53396 to D.J. Klionsky.

Submitted: 7 January 2008
Accepted: 23 July 2008

References

Bowers, K., and T.H. Stevens. 2005. Protein transport from the late Golgi to the vacuole in the yeast *Saccharomyces cerevisiae. Biochim. Biophys. Acta.* 1744:438–454.

Cao, Y., and D.J. Klionsky. 2007. Physiological functions of Atg6/Beclin 1: a unique autophagy-related protein. *Cell Res.* 17:839–849.

Cheong, H., T. Yorimitsu, F. Reggiori, J.E. Legakis, C.-W. Wang, and D.J. Klionsky. 2005. Atg17 regulates the magnitude of the autophagic response. *Mol. Biol. Cell.* 16:3438–3453.

Cheong, H., U. Nair, J. Geng, and D.J. Klionsky. 2008. The Atg1 kinase complex is involved in the regulation of protein recruitment to initiate sequestering vesicle formation for nonspecific autophagy in *Saccharomyces cerevisiae. Mol. Biol. Cell.* 19:668–681.

Dove, S.K., R.C. Piper, R.K. McEwen, J.W. Yu, M.C. King, D.C. Hughes, J. Thuring, A.B. Holmes, F.T. Cooke, R.H. Michell, et al. 2004. Svp1p defines a family of phosphatidylinositol 3,5-bisphosphate effectors. *EMBO J.* 23:1922–1933.

Fujioka, Y., N.N. Noda, K. Fujii, K. Yoshimoto, Y. Ohsumi, and F. Inagaki. 2008. In vitro reconstitution of plant ATG8 and ATG12 conjugation systems essential for autophagy. *J. Biol. Chem.* 283:1921–1928.

Gerhardt, B., T.J. Kordas, C.M. Thompson, P. Patel, and T. Vida. 1998. The vesicle transport protein Vps33p is an ATP-binding protein that localizes to the cytosol in an energy-dependent manner. *J. Biol. Chem.* 273:15818–15829.

Guan, J., P.E. Stromhaug, M.D. George, P. Habibzadegah-Tari, A. Bevan, W.A. Dunn Jr., and D.J. Klionsky. 2001. Cvt18/Gsa12 is required for cytoplasm-to-vacuole transport, pexophagy, and autophagy in *Saccharomyces cerevisiae* and *Pichia pastoris. Mol. Biol. Cell.* 12:3821–3838.

Gueldener, U., J. Heinisch, G.J. Koehler, D. Voss, and J.H. Hegemann. 2002. A second set of loxP marker cassettes for Cre-mediated multiple gene knockouts in budding yeast. *Nucleic Acids Res.* 30:e23.

Hanada, T., N.N. Noda, Y. Satomi, Y. Ichimura, Y. Fujioka, T. Takao, F. Inagaki, and Y. Ohsumi. 2007. The ATG12-ATG5 conjugate has a novel E3-like activity for protein lipidation in autophagy. *J. Biol. Chem.* 282:37298–37302.

Huang, W.-P., S.V. Scott, J. Kim, and D.J. Klionsky. 2000. The itinerary of a vesicle component, Aut7p/Cvt5p, terminates in the yeast vacuole via the autophagy/Cvt pathways. *J. Biol. Chem.* 275:5845–5851.

Ichimura, Y., T. Kirisako, T. Takao, Y. Satomi, Y. Shimonishi, N. Ishihara, N. Mizushima, I. Tanida, E. Kominami, M. Ohsumi, et al. 2000. A ubiquitin-like system mediates protein lipidation. *Nature.* 408:488–492.

Ichimura, Y., Y. Imamura, K. Emoto, M. Umeda, T. Noda, and Y. Ohsumi. 2004. *In vivo* and *in vitro* reconstitution of Atg8 conjugation essential for autophagy. *J. Biol. Chem.* 279:40584–40592.

Iwata, J., J. Ezaki, M. Komatsu, S. Yokota, T. Ueno, I. Tanida, T. Chiba, K. Tanaka, and E. Kominami. 2006. Excess peroxisomes are degraded by autophagic machinery in mammals. *J. Biol. Chem.* 281:4035–4041.

Kabeya, Y., T. Kawamata, K. Suzuki, and Y. Ohsumi. 2007. Cis1/Atg31 is required for autophagosome formation in *Saccharomyces cerevisiae. Biochem. Biophys. Res. Commun.* 356:405–410.

Kawamata, T., Y. Kamada, Y. Kabeya, T. Sekito, and Y. Ohsumi. 2008. Organization of the pre-autophagosomal structure responsible for autophagosome formation. *Mol. Biol. Cell.* 19:2039–2050.

Kim, J., S.V. Scott, M.N. Oda, and D.J. Klionsky. 1997. Transport of a large oligomeric protein by the cytoplasm to vacuole protein targeting pathway. *J. Cell Biol.* 137:609–618.

Kim, J., Y. Kamada, P.E. Stromhaug, J. Guan, A. Hefner-Gravink, M. Baba, S.V. Scott, Y. Ohsumi, W.A. Dunn Jr., and D.J. Klionsky. 2001. Cvt9/Gsa9 functions in sequestering selective cytosolic cargo destined for the vacuole. *J. Cell Biol.* 153:381–396.

Klionsky, D.J. 2005. The molecular machinery of autophagy: unanswered questions. *J. Cell Sci.* 118:7–18.

Klionsky, D.J. 2007. Autophagy: from phenomenology to molecular understanding in less than a decade. *Nat. Rev. Mol. Cell Biol.* 8:931–937.

Klionsky, D.J., R. Cueva, and D.S. Yaver. 1992. Aminopeptidase I of *Saccharomyces cerevisiae* is localized to the vacuole independent of the secretory pathway. *J. Cell Biol.* 119:287–299.

Kuma, A., N. Mizushima, N. Ishihara, and Y. Ohsumi. 2002. Formation of the approximately 350-kDa Apg12-Apg5·Apg16 multimeric complex, mediated by Apg16 oligomerization, is essential for autophagy in yeast. *J. Biol. Chem.* 277:18619–18625.

Levine, B., and D.J. Klionsky. 2004. Development by self-digestion: molecular mechanisms and biological functions of autophagy. *Dev. Cell.* 6:463–477.

Longtine, M.S., A. McKenzie III, D.J. Demarini, N.G. Shah, A. Wach, A. Brachat, P. Philippsen, and J.R. Pringle. 1998. Additional modules for versatile and economical PCR-based gene deletion and modification in *Saccharomyces cerevisiae. Yeast.* 14:953–961.

Mizushima, N. 2007. Autophagy: process and function. *Genes Dev.* 21:2861–2873.

Mizushima, N., T. Noda, T. Yoshimori, Y. Tanaka, T. Ishii, M.D. George, D.J. Klionsky, M. Ohsumi, and Y. Ohsumi. 1998. A protein conjugation system essential for autophagy. *Nature.* 395:395–398.

Mizushima, N., T. Noda, and Y. Ohsumi. 1999. Apg16p is required for the function of the Apg12p-Apg5p conjugate in the yeast autophagy pathway. *EMBO J.* 18:3888–3896.

Robinson, J.S., D.J. Klionsky, L.M. Banta, and S.D. Emr. 1988. Protein sorting in *Saccharomyces cerevisiae*: isolation of mutants defective in the delivery and processing of multiple vacuolar hydrolases. *Mol. Cell. Biol.* 8:4936–4948.

Rubinsztein, D.C., J.E. Gestwicki, L.O. Murphy, and D.J. Klionsky. 2007. Potential therapeutic applications of autophagy. *Nat. Rev. Drug Discov.* 6:304–312.

Scherz-Shouval, R., E. Shvets, E. Fass, H. Shorer, L. Gil, and Z. Elazar. 2007. Reactive oxygen species are essential for autophagy and specifically regulate the activity of Atg4. *EMBO J.* 26:1749–1760.

Scott, S.V., J. Guan, M.U. Hutchins, J. Kim, and D.J. Klionsky. 2001. Cvt19 is a receptor for the cytoplasm-to-vacuole targeting pathway. *Mol. Cell.* 7:1131–1141.

Shao, Y., Z. Gao, T. Feldman, and X. Jiang. 2007. Stimulation of ATG12-ATG5 conjugation by ribonucleic acid. *Autophagy.* 3:10–16.

Shintani, T., and D.J. Klionsky. 2004. Cargo proteins facilitate the formation of transport vesicles in the cytoplasm to vacuole targeting pathway. *J. Biol. Chem.* 279:29889–29894.

Shintani, T., W.-P. Huang, P.E. Stromhaug, and D.J. Klionsky. 2002. Mechanism of cargo selection in the cytoplasm to vacuole targeting pathway. *Dev. Cell.* 3:825–837.

Sikorski, R.S., and P. Hieter. 1989. A system of shuttle vectors and yeast host strains designed for efficient manipulation of DNA in *Saccharomyces cerevisiae. Genetics.* 122:19–27.

Stromhaug, P.E., F. Reggiori, J. Guan, C.-W. Wang, and D.J. Klionsky. 2004. Atg21 is a phosphoinositide binding protein required for efficient lipidation and localization of Atg8 during uptake of aminopeptidase I by selective autophagy. *Mol. Biol. Cell.* 15:3553–3566.

Suzuki, K., T. Kirisako, Y. Kamada, N. Mizushima, T. Noda, and Y. Ohsumi. 2001. The pre-autophagosomal structure organized by concerted functions of *APG* genes is essential for autophagosome formation. *EMBO J.* 20:5971–5981.

Suzuki, K., Y. Kubota, T. Sekito, and Y. Ohsumi. 2007. Hierarchy of Atg proteins in pre-autophagosomal structure organization. *Genes Cells.* 12:209–218.

Yorimitsu, T., and D.J. Klionsky. 2005. Atg11 links cargo to the vesicle-forming machinery in the cytoplasm to vacuole targeting pathway. *Mol. Biol. Cell.* 16:1593–1605.

Zheng, L., U. Baumann, and J.-L. Reymond. 2004. An efficient one-step site-directed and site-saturation mutagenesis protocol. *Nucleic Acids Res.* 32:e115.